Available online at www.sciencedirect.com
ScienceDirect
Scripta Materialia 64 (2011) 832–835
Scripta MATERIALIA
www.elsevier.com/locate/scriptamat

Improvement in the mechanical performance of Czochralski silicon under indentation by germanium doping

Zhidan Zeng,[a] Lin Wang,[b,c] Xiangyang Ma,[a] Shaoxing Qu,[d] Jiahe Chen,[a] Yonggang Liu[e] and Deren Yang[a,*]

[a] *State Key Laboratory of Silicon Materials and Department of Materials Science and Engineering, Zhejiang University, Hangzhou 310027, People's Republic of China*
[b] *High Pressure Synergetic Consortium (HPSynC), Geophysical Laboratory, Carnegie Institution of Washington, Argonne, IL 60439, USA*
[c] *State Key Laboratory of Superhard Materials, Jilin University, Changchun 130012, People's Republic of China*
[d] *Institute of Applied Mechanics,School of Aeronautics and Astronautics, Zhejiang University, Hangzhou 310027, People's Republic of China*
[e] *Institute of Geochemistry, Chinese Academy of Sciences, Guiyang 550002, People's Republic of China*

Received 22 October 2010; revised 9 January 2011; accepted 10 January 2011
Available online 13 January 2011

The mechanical properties of germanium-doped Czochralski (GCz) silicon have been investigated using instrumented nanoindentation combined with an ultrasonic pulse-echo overlap technique. The GCz silicon samples showed higher Young's modulus and hardness than germanium-free Czochralski silicon samples in nanoindentation tests. We believe this was caused by the enhanced phase transition from the Si-I phase to the stiffer Si-II phase in GCz silicon under contact load during indentation. This scenario was further confirmed by micro-Raman spectroscopy measurements.
© 2011 Acta Materialia Inc. Published by Elsevier Ltd. All rights reserved.

Keywords: Silicon; Nanoindentation; Phase transformation; Raman spectroscopy; Germanium doping

Czochralski (Cz) silicon has been widely employed in the fabrication of integrated circuits, microelectromechanical systems, and infrared optic and photovoltaic devices. However, the brittleness of silicon could lead to strength-degrading cracks during device manufacture since it is frequently subjected to localized high stress at micro- and nanometer scales, which influences the manufacturing yield, device performance and reliability [1]. Moreover, with the trend of increasing wafer diameters, maintaining and improving the mechanical strength of silicon wafers have become especially critical as increasing thermal and gravitational stresses might cause slip and warpage of wafers during manufacture [2,3]. Intentional doping with impurities such as nitrogen and germanium has been proposed to improve the mechanical strength of silicon wafers [4–6]. In the past, wafer warpage and dislocation movement were reported to be suppressed by germanium doping, and enhanced fracture toughness was also observed in annealed germanium-doped Czochralski (GCz) silicon [6]. However, the mechanical properties of GCz silicon at nanometer scales are still unknown.

As one of the most common mechanical impacts that a Cz silicon wafer experiences during manufacture, contact loading can cause surface damage and phase transformations under localized high stresses [7–10]. Nanoindentation with unique load–depth sensing capabilities has been successfully and extensively employed to investigate the mechanical response of materials during contact loading at nanometer scales [11–14]. In this work, we investigated the mechanical properties of GCz (with a germanium doping level of $\sim10^{19}$ cm^{-3}) and Cz silicon using nanoindentation. It was found that GCz silicon showed a stiffer behavior under contact loading during nanoindentation than Cz silicon. Micro-Raman spectroscopy and an ultrasonic pulse-echo overlap method were further employed to investigate the origin of the enhanced mechanical properties of GCz silicon.

The samples prepared in this study were (1 0 0)-oriented GCz and Cz silicon with almost the same interstitial oxygen concentrations ($9.2–9.4 \times 10^{17}$ cm^{-3}),

* Corresponding author. E-mail: mseyang@zju.edu.cn

1359-6462/$ - see front matter © 2011 Acta Materialia Inc. Published by Elsevier Ltd. All rights reserved.
doi:10.1016/j.scriptamat.2011.01.014

measured by Fourier transform infrared spectroscopy with a calibration coefficient of 3.14×10^{17} cm^{-2}. The germanium concentration in GCz silicon was about 8×10^{19} cm^{-3} (about 0.2 at.%) measured by secondary ion mass spectrometry. The samples were all treated by RCA cleaning, then dipped into dilute HF for 5 min to remove the oxide layer, followed by a thorough rinse in deionized water. Nanoindentation tests were performed using a nanotriboindenter (Hysitron Inc., USA) with a Berkovich diamond indenter. A maximum load F_{max} of 10 mN was applied with a constant loading/unloading rate of 0.05 mN s^{-1}. The holding time at F_{max} was 30 s to minimize the time-dependent plastic effect. The orientations of these samples with respect to the indenter were kept identical in the experiments, with the Si [1 1 0] direction parallel to one face of the indenter. The tests were repeated several times on different samples at different times to avoid accidental artifacts.

Indentation-induced structure changes in both the specimens were investigated using a micro-Raman spectrometer (Renishaw, UK) with an Ar^+ laser (excitation wavelength 514 nm). A 50× objective was used to focus the laser beam, with the beam size being about 4 μm. The laser power was 24 mW, with a collection time of 60 s. This gives a power density of approximately 190 kW cm^{-2}, comparable to the power density of the 514 nm laser used in other work in which the laser heating effect was suggested to be negligible [8,15]. All micro-Raman spectroscopy measurements were performed under the same conditions. For each sample, Raman spectra were acquired on 10 indents, which were produced by a Vickers microindenter with a load of 10 g and a loading/unloading rate of approximately 30 mN s^{-1}. An ultrasonic pulse-echo overlap method [16] was employed to derive the Young's modulus of GCz and Cz silicon specimens by measuring the velocities of longitudinal and transverse waves propagating along the [1 0 0] of specimens, using a Panametric 5900 pulser/receiver instrument.

The load–displacement curves (*P–h* curves) of the GCz and Cz specimens are shown in Figure 1(a). The GCz and Cz silicon specimens show similar *P–h* curves with continuous loading segments and pop-out in unloading segments. Both the loading and unloading segments of the GCz silicon in Figure 1(a) show sharper slopes than those of the germanium-free Cz silicon.

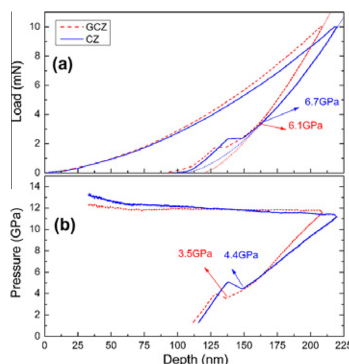

Figure 1. Nanoindentation tests of Cz and GCz silicon specimens. (a) *P–h* curves of the Cz silicon (solid blue line) and GCz silicon (dashed red line) specimens, with a maximum load of 10 mN and a constant loading/unloading rate of 0.05 mN s^{-1}. The dotted lines represent the power-law fitting of the initial unloading *P–h* curves. (b) Corresponding average contact pressure vs. the depth curves of (a).

The loading segment generally includes both elastic and plastic deformation. Herein the plastic deformation is dominated by the phase transition from the cubic Si-I phase to the metallic β-Sn Si-II phase beneath the indenter during loading rather than dislocation as the load is quite low [17]. The metallic phase transition of silicon generally occurs at a hydrostatic pressure of 11.3–12.5 GPa [18]. Under non-hydrostatic pressure, the transition pressure will decrease due to shear stress, e.g. in the case of indentation [19,20]. Indentation with various loads, from a very low load of several micronewtons to several hundred millinewtons, can induce pressures of the magnitude needed to cause this phase transition in silicon [21–24].

During unloading, depending on the F_{max}, the unloading rate, etc. [25,26], the Si-II phase can further transform to Si-III and Si-XII phases or the amorphous phase *a*-Si. The former transformation generally causes a pop-out effect during unloading, with a high F_{max} and low unloading rate; in contrast, the latter one results in an elbow event, with a low F_{max} and high unloading rate [12,22,25]. For the F_{max} of 10 mN and unloading rate of 0.05 mN s^{-1} used in this work, pop-out effects generally occur in Cz silicon [25,26], which is consistent with the results in this work, even with similar slopes in the *P–h* curves [26]. Moreover, pop-out effects were also observed in the GCz silicon samples, implying similar phase transitions.

The maximum indentation displacement h_{max} in the Cz silicon is about 10 nm deeper than that in the GCz silicon. However, the residual indentation depths of these two samples are very close. The initial unloading deformations in nanoindentations of both the GCz and Cz silicon samples are purely elastic as they perfectly follow the power-law relation [27]:

$$F = \alpha(h - h_r)^m \quad (1)$$

where F is the load, h is the depth, h_r is the residual depth after the complete unloading, α is material constant and m is related to shape of the indenter. Such deformation characteristics mean that the high-pressure metallic phase Si-II that developed in the loading process remains stable at the initial unloading stage when the indentation pressure is still high, leading to an overall elastic response of both Si-I and Si-II phases [28]. In Figure 1(a), the dotted lines represent the power-law relation fittings, which show a clearly sharper slope and a smaller elastic recovery in the GCz than that in the Cz silicon.

The relative modulus (E_r) can be extracted from the unloading–displacement data (in Fig. 1(a)) using the Oliver–Pharr method [27]. The Young's modulus of the specimens can then be calculated according to:

$$\frac{1}{E_r} = \frac{1 - v^2}{E} + \frac{1 - v_i^2}{E_i} \quad (2)$$

where E and v are the Young's modulus and Poisson's ratio for the samples and E_i and v_i are that for the indenter, respectively. For the diamond indenter, $E_i = 1141$ GPa and $v_i = 0.07$, and for silicon, $v = 0.3$ [27]. The Young's modulus of the GCz and Cz silicon samples were found to be 153.8 ± 4.1 and 136.7 ± 7.2 GPa, respectively. (The absolute values of Young's modulus of silicon vary by tens of gigapascals in different measurements [26,29]; we therefore concentrated on the

relative differences between GCz and Cz using the same measurements in this work.)

As a non-destructive technique, the ultrasonic pulse-echo overlap method has been extensively used for the accurate measurements of moduli of all kinds of bulk materials [16]. Here we employed it to measure the modulus of the GCz and Cz silicon samples. Ultrasonic measurements showed that the Young's modulus of the GCz silicon is just 0.4% lower than that of the Cz silicon. Theoretical calculations suggest that the Young's modulus of SiGe alloys decreases linearly with increasing germanium concentration [30]. As the germanium concentration is less than 0.2% in the GCz silicon used in this work, the relative change in Young's modulus is estimated to be of the same order as the germanium concentration, which is consistent with the results of the ultrasonic measurements. However, according to the nanoindentation results, the Young's modulus of GCz silicon is surprisingly about 13% higher than that of Cz silicon. During the loading stage, part of the Si-I phase beneath the indenter transformed to the Si-II phase, with a much higher Young's modulus of about 304 GPa [31]. Therefore, it is reasonable to assume that the higher Young's modulus of the GCz silicon extracted in the nanoindentation tests is caused by the larger amount of the Si-II phase developed in the GCz silicon. This can be seen in the observed stiffer behavior of GCz silicon in the *P*–*h* curves with a smaller h_{max}, a sharper slope in the unloading segment and a smaller elastic displacement recovery.

Using the elastic theory of contact mechanics [12,27,32], the dependence of the average contact pressure on indentation depth throughout the loading and unloading processes was calculated (see Fig. 1(b)). Herein the area function for the indenter is $A_i = 24.5h_c^2 + 1378h_c$, where A_i is the contact area and h_c is the contact depth. The average hardness value (corresponding to the pressure at F_{max}[19] in Fig. 1(b)) of GCz silicon (12.5 GPa) is higher than in Cz silicon (11.3 GPa).

The bifurcations of the unloading curve from the dotted fitting lines generally indicate the onset of phase transformation from the Si-II phase to the Si-III and/or Si-XII phases [12]. The bifurcation pressure of GCz silicon is 6.1 GPa, lower than 6.7 GPa of Cz silicon, which indicates that the Si-II phase in GCz silicon seems to be more stable than that in Cz silicon during unloading. This implies that germanium doping could promote and stabilize the metallic Si-II phase under indentation.

Micro-Raman spectroscopy was further employed to investigate the metallic phase transformation in the Cz and GCz silicon samples during indentations. Previous Raman investigations suggest that the Si-I peak will shift to a lower wavenumber in the SiGe alloy and the peak shift is proportional to the Ge fraction in the alloy [33,34]. However, in this work, the influence of Ge doping on Raman spectrum of silicon can be ignored as the Ge concentration is very low (about 0.2% in our GCz silicon), which will cause peak shift of approximate 0.14 cm^{-1}, estimated according to the empirical equations in the literature [33,34]. This 0.14 cm^{-1} peak shift is too small to show an obvious difference.

Figure 2(a) shows the Raman spectra for undeformed Cz and GCz silicon (without indentation), in which the two spectra almost coincide with each other, consistent

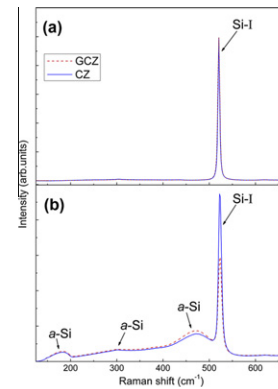

Figure 2. Micro-Raman spectra for germanium-free Cz silicon (solid blue line) and GCz silicon (dashed red line) on undeformed area (a) and residual impressions (b). For each sample, 10 residual impressions were produced by a Vickers indentation with a load of 10 g and a loading/unloading rate of approximately 30 mN s^{-1}, and the micro-Raman spectra were obtained by averaging the 10 spectra.

with the above-mentioned low-doping-concentration viewpoint. Microindentation with bigger impressions and the same phase transitions during loading [9] was chosen to produce indents instead of nanoindentations. The metastable Si-II phase developed during the loading in microindentation is reported to transform totally into *a*-Si phase during unloading when the unloading rate is very high [9,15,23]. Therefore, the amount of the Si-II phase produced during loading can be conveniently estimated according to the amount of *a*-Si after unloading in the relative big residual microimpressions.

Figure 2(b) shows the averaged Raman spectra of 10 tests in the Cz and GCz silicon samples. These two spectra both show a sharp peak at about 522 cm^{-1} corresponding to the Si-I phase and three broad peaks around 170, 300, 470 cm^{-1} as the characteristic Raman bands of the *a*-Si phase [35,36]. The laser beam (4 μm in diameter) can cover the whole residual indentation impression (about 3 μm in lateral dimensions in both the GCz and Cz silicon samples) completely with a constant penetration depth (about 150 nm in *a*-Si region) [32,37]. Since the penetration depth is less than the largest depth of *a*-Si (approximate 500 nm, estimated according to TEM results in indents with a similar load in Ref. [23]), the intensities of the *a*-Si Raman peaks reflect the relative amount of *a*-Si phase in the horizontal direction in the indentation area. The change in this relative amount can reflect the change in absolute volume of *a*-Si induced by each indentation, as the *a*-Si distribution will expand in both horizontal and depth directions when the total *a*-Si amount increases.

As can be seen in Figure 2(b), the peaks of the *a*-Si phase in the GCz silicon are clearly stronger than that in the Cz silicon, while the peaks of the Si-I phase are much weaker, with perfectly consistent backgrounds. The difference in peak intensity between the GCz and Cz silicon suggests that more Si-II phase has developed at the expense of Si-I phase during indentation in the GCz silicon. This is consistent with the result showing the lower destabilization pressure of Si-II in the GCz silicon than in the Cz silicon observed in the nanoindentation tests described above. These results imply that the metallic phase transformation from the Si-I phase to

the Si-II phase in the GCz silicon samples is enhanced compared with the Cz silicon samples.

The silicon extensively used in industry is doped with impurities, and the effects of these impurities on the phase transitions in silicon under contact load have been of significant importance and interest [38]. Germanium was reported to alter the Si-I to Si-II phase transition pressure in SiGe alloys with high germanium concentration in diamond anvil cells (DAC); for example, for $Si_{0.103}Ge_{0.897}$, the phase transition pressure is $\sim$11.5 GPa ($\sim$12.6 GPa in pure silicon) [39]. Here we showed a remarkable promotion effect on the Si-I to Si-II phase transition under indentation in GCz silicon, which is surprising because of the low doping concentration of germanium (about 0.2%). As this transition is very sensitive to the shear stress [17,39] and the sharp contact load in indentation causes high non-hydrostatic and deviatoric stresses, the phase transition in indentation may be different from that in DAC. The enhanced metallic phase transition in GCz may be related to the chemical stress induced by germanium doping in the silicon. However, the details require more investigation, including experiments and computations. As the entire concept of ductile regime machining (an ultra-precision machining process applied by the semiconductor industry) is based on the transformation from the brittle (Si-I) to the ductile (Si-II) phase [40], our results may provide a new approach to improving the mechanical performance of silicon wafers by germanium doping at micro- and nanometer scales.

In conclusion, the mechanical behavior of GCz silicon wafers has been investigated by nanoindentation, with Cz silicon wafers tested as controls. A stiffer mechanical behavior with smaller h_{max}, higher hardness and larger Young's modulus was observed in GCz silicon compared with Cz silicon. The improvement was suggested to be caused by the promotion effect of germanium doping on metallic phase transformation (Si-I to Si-II phases) during indentation, which was further confirmed by micro-Raman spectroscopy measurements. These results may also provide a new approach to improving the mechanical performance of silicon wafers under contact loading at micro- and nanometer scales.

The authors thank the following for financial support: Natural Science Foundation of China (Nos. 50832006, 60876001, 60906001 and 50672085), Program PCSIT, Program 973 (No. 2007CB613403) and the Research Fund for the Doctoral Program of Higher Education (No. 200803350043). The authors also thank Dr. John Murphy from University of Oxford for valuable discussion, and Dr. Yugang Sun and David J. Gosztola for experimental help. L.W. is grateful for the support from Efree, an Energy Frontier Research Center funded by the DOE, Office of Science and Office of Basic Energy Sciences under Award No. DE-SC0001057. Part of this work was conducted at the Center for Nanoscale Materials at ANL (Contract No. DE-AC02-06CH11357).

[1] S.Y. Luo, Z.W. Wang, Int. J. Adv. Manuf. Technol. 35 (2008) 1206.
[2] A. Fischer, G. Kissinger, Appl. Phys. Lett. 91 (2007) 111911.
[3] Z.H. Gan, C.M. Tan, Microelectron. Eng. 71 (2004) 150.
[4] I. Yonenaga, J. Appl. Phys. 98 (2005) 023517.
[5] C.R. Alpass, J.D. Murphy, R.J. Falster, P.R. Wilshaw, J. Appl. Phys. 105 (2009) 013519.
[6] J.H. Chen, D.R. Yang, X.Y. Ma, Z.D. Zeng, D.X. Tian, L.B. Li, D.L. Que, L.F. Gong, J. Appl. Phys. 103 (2008) 123521.
[7] L.C. Zhang, I. Zarudi, Int. J. Adv. Manuf. Technol. 43 (2001) 1985.
[8] J.W. Yan, H. Takahashi, J. Tamaki, X.H. Gai, H. Harada, J. Patten, Appl. Phys. Lett. 86 (2005) 181913.
[9] A. Kailer, Y.G. Gogotsi, K.G. Nickel, J. Appl. Phys. 81 (1997) 3057.
[10] Y.Q. Wu, H. Huang, J. Zou, L.C. Zhang, J.M. Dell, Scr. Mater. 63 (2010) 847.
[11] S. Ruffell, J.E. Bradby, J.S. Williams, D. Munoz-Paniagua, S. Tadayyon, L.L. Coatsworth, P.R. Norton, Nanotechnology 20 (2009) 135603.
[12] L. Chang, L.C. Zhang, Acta Mater. 57 (2009) 2148.
[13] G. Feng, W.D. Nix, Y. Yoon, C.J. Lee, J. Appl. Phys. 99 (2006) 074304.
[14] Y. Lu, Y. Ganesan, J. Lou, Exp. Mech. 50 (2010) 47.
[15] G. Lucazeau, L. Abello, J. Mater. Res. 12 (1997) 2262.
[16] E.P. Papadaki, J. Acoust. Soc. Am. 42 (1967) 1045.
[17] I. Zarudi, J. Zou, L.C. Zhang, Appl. Phys. Lett. 82 (2003) 874.
[18] J.Z. Hu, L.D. Merkle, C.S. Menoni, I.L. Spain, Phys. Rev. B 34 (1986) 4679.
[19] J.J. Gilman, Philos. Mag. B 67 (1993) 207.
[20] K. Gaal-Nagy, D. Strauch, Phys. Rev. B 73 (2006).
[21] K. Mylvaganam, L.C. Zhang, P. Eyben, J. Mody, W. Vandervorst, Nanotechnology 20 (2009) 305705.
[22] J.E. Bradby, J.S. Williams, M.V. Swain, Phys. Rev. B 67 (2003) 085205.
[23] J.E. Bradby, J.S. Williams, J. Wong-Leung, M.V. Swain, P. Munroe, J. Mater. Res. 16 (2001) 1500.
[24] S.J. Lloyd, J.M. Molina-Aldareguia, W.J. Clegg, J. Mater. Res. 16 (2001) 3347.
[25] V. Domnich, Y. Gogotsi, S. Dub, Appl. Phys. Lett. 76 (2000) 2214.
[26] J.I. Jang, M.J. Lance, S.Q. Wen, T.Y. Tsui, G.M. Pharr, Acta Mater. 53 (2005) 1759.
[27] W.C. Oliver, G.M. Pharr, J. Mater. Res. 7 (1992) 1564.
[28] W.C.D. Cheong, L.C. Zhang, Nanotechnology 11 (2000) 173.
[29] Y.B. Gerbig, S.J. Stranick, D.J. Morris, M.D. Vaudin, R.F. Cook, J. Mater. Res. 24 (2009) 1172.
[30] F. Schaffler, Properties of Advanced Semiconductor Materials GaN, AlN, InN, BN, SiC, SiGe, John Wiley & Sons, New York, 2001.
[31] T. Kiriyama, H. Harada, J.W. Yan, Semicond. Sci. Technol. 24 (2009) 025014.
[32] T. Juliano, Y. Gogotsi, V. Domnich, J. Mater. Res. 18 (2003) 1192.
[33] J.C. Tsang, P.M. Mooney, F. Dacol, J.O. Chu, J. Appl. Phys. 75 (1994) 8098.
[34] F. Pezzoli, L. Martinelli, E. Grilli, A. Guzzi, S. Sanguinetti, M. Bollani, H.D. Chrastina, G. Isella, H. von Kanel, E. Wintersberger, J. Stangl, G. Bauer, Mater. Sci. Eng. B 124 (2005) 127.
[35] K.H. Wu, X.Q. Yan, M.W. Chen, Appl. Phys. Lett. 91 (2007) 101903.
[36] B. Haberl, A.C.Y. Liu, J.E. Bradby, S. Ruffell, J.S. Williams, P. Munroe, Phys. Rev. B 79 (2009) 155209.
[37] A.J. Scholten, A.V. Akimov, J.I. Dijkhuis, Phys. Rev. B 54 (1996) 12151.
[38] X.Q. Yan, X.M. Huang, S. Uda, M.W. Chen, Appl. Phys. Lett. 87 (2005) 191911.
[39] A. Werner, J.A. Sanjurjo, M. Cardona, Solid State Commun. 44 (1982) 155.
[40] J. Patten, H. Cherukuri, J. Yan, in: Y. Gogotsi, V. Domnich (Eds.), High Pressure Surface Science and Engineering, Institute of Physics, Bristol, 2004, p. 542.